Platelet-activating Factor Acetyl Hydrolase IB2 Dysregulated Cell Proliferation in Ovarian Cancer

yingying he
Yunnan University
zhicheng he
Kunming Institute of Botany Chinese Academy of Sciences
Xiaoyu Zhang
Kunming Institute of Botany Chinese Academy of Sciences
SHUBAI LIU (liushubai@mail.kib.ac.cn)
Kunming Institute of Botany Chinese Academy of Sciences https://orcid.org/0000-0001-8929-4209

Primary research

Keywords: Platelet-activating factor acetylhydrolase 1B2, ovarian cancer, ester lipid, tyrosine kinase signaling pathway, Platelet-activating factor

Posted Date: November 2nd, 2021

DOI: https://doi.org/10.21203/rs.3.rs-1027844/v1

Version of Record: A version of this preprint was published at Cancer Cell International on December 1st, 2021. See the published version at https://doi.org/10.1186/s12935-021-02406-9.

Abstract

Background

Ovarian cancer is the world's largest cause of death for gynaecologic diseases. Platelet-activating factor acetyl hydrolase IB2 (PAF-AH IB2) is an intracellular serine esterase that hydrolyzes platelet-activating factor, a G-protein-like trimer with two catalytic subunits and one regulatory subunit. The deregulatory role of PAF-AHIB2 in the etiology of ovarian cancer is poorly understood.

Methods

In this study, the TCGA exploration and cancer tissue immunohistochemistry were utilized to investigate aberrant overexpression of PAF-AH IB2 in ovarian cancer. PAF-AH IB2 Stable knocking down (KD) ovarian cancer cells were established to investigate the impact on the cell proliferation, migration, and tumorigenicity in vitro. The whole transcription profiling, tyrosine kinase profiling and standard cell functional assays were integrated to explore the biological importance and mechanism of PAF-AH IB2 modulated in ovarian cancer.

Results

Interesting, PAF-AH IB2 was identified significantly overexpression in four subtypes of ovarian cancer. PAF-AHIB2 KD significantly reduced cancer cell proliferation, migration, and tumorigenicity in vitro, activated Caspases and caused cell cycle arrest, and making the cells more sensitive to PAF. Several key regulators of multiple tyrosine kinases-mediated signaling pathway were down-regulated in PAF-AH 1B2 KD cells, revealing a novel interaction network between the growth factor receptors pathway and PAF-AH 1B2 mediated PAF signalling.

Conclusions

These results discovered an unrevealed role for PAFAH IB2 as a novel potential therapy target and essential signaling mediators in ovarian cancer pathogenesis, as well as new potential preventive and therapeutic strategies to inhibit this enzyme in clinical treatment for ovarian cancer.

Background

Ovarian carcer is the gynaecological malignancy with the highest death rate among gynaecological cancers. The epithelial serous cancer, the most common epithelial ovarian malignancy, has a 5-year survival rate of less than 25% and a 10-year survival rate approaching zero [1]. The later stage of disease diagnosis and lack of effective therapy strategy contribute to the higher death rate of ovarian cancer. Therefore, it is very urgently need to develop the disease-specific, target therapy approaches to improve the survival of ovarian carcinoma. It is important to enhance the understand the mechanism of ovarian cancer and discover the key molecules that associated with malignant transformation and carcinogenesis.

Esterase enzymes are a subclass of the hydrolase enzyme superfamily that specifically hydrolyse ester bonds [2, 3]. Multiple types of esterases have been identified based on differences in substrate specificity and biological function, and some esterases have been found to be dysregulated and overexpressed in cancer cells [3, 4]. Esterase enzymes have been linked to metabolic pathway reprogramming, cancer pathogenesis, drug metabolism, and drug toxicity [2, 3]. Platelet-activating factor acetyl hydrolases (PAF-AHs) are phospholipase A2 family serine esterases that cleave the sn-2 active side chain to hydrolyze Platelet-activating factor (PAF), which is involved in many reproductive physiology roles, such as fertilization and parturition [5, 6]. PAF-AH IB is a tissue (intracellular) type with no sequence homology to other PAF-AHs in group VII. PAF is the only identified substrate of the type I PAF acetyl hydrolase in tissue [7]. PAF-AH IB is a G-protein-like trimer composed of two 29-kDa 1 (also known as PAF-AH IB3) and 2 (30 kDa) (PAF-AH IB2) catalytic subunits that form homodimers or heterodimers and sharing ~63% sequence identity, formed homodimers or heterodimers, and worked as a complex with a noncatalytic 45-kDa regulatory beta subunit, LIS1 [8-10]. In human, α2 is ubiquitously with higher expressed in brain, kidney, spleen, et al, while with little expression in heart, lung and ovarian et al [11]. The intracellular activity of PAF-AH 1B was decreased in rat uterine myometrium due to the protein expression change and the level of PAF increase in later stage of pregnancy [12]. Platelet-activating factor acetyl hydrolases 1B2 and 1B3 are poorly characterized serine hydrolases, which could form a protein complex with a non-catalytic protein (Lis1) and regulate brain development, spermatogenesis, and cancer pathogenesis[9]. Pregnancy-induced hypertension is caused by abnormal, unregulated PAF-AH 1B activity [13, 14]. These findings suggest that PAF-AH 1B may play an important role in the maintenance of homeostasis by degrading PAF. However, it's little known that the precise role and regulated molecular mechanism of platelet activating factor-acetyl hydrolase IB act in ovarian pathogenesis.

Here, we integrated application of whole transcription profiling, tyrosine kinase profiling technologies as well as standard functional assays to explore the biological significance and pathways of PAF-AH IB2 in ovarian cancer. These results will be helpful to define the role of PAF-AH IB2 in ovarian cancer pathogenesis.

Methods

Plasmids and transfection

The human PAFAH IB2 full length expression plasmid (pEGFP-C1-PAF-AHIB2-WT) was got as gift from Prof. Xueliang Zhu [15] and used to co-express GFP as a marker. The mouse PAFAH IB2 WT, functional mutants (E39D, S48C, E39D/S48C) and Lis1(pcDNA3.1-3xFlag vector) were bought from NovoPro and confirmed by sequencing. The HOSE (1 x 10^3) cells growing in complete medium were transfected with human PAFAH IB2 and mouse PAFAH IB2 wild type and mutant constructs for relative functional assay.

Explore PAF-AH IB2 gene with ovarian carcinoma cases through TCGA

The PAF-AH IB2 genes were explored in the Cancer Genomics dataset (TCGA) through Gepia and investigated the genetic alterations associated with serous ovarian carcinoma's patient's cases, which provides large-scale cancer patients genomics data sets from TCGA to research community for visualization, analysis and downloads [16]. Kaplan–Meier plots were generated from an online dataset (http://www.kmplot.com) [GSE15459 and GSE62254]. The disease-free survival (PFS) analysis was performed by using patient's information. The patient's population was split by median value.

Ovarian Cancer Cell lines

The human ovarian cancer cell lines, represent the Endometrioid (Tov112D), Clear cells (RMG1), Serious (SKOV3, OVCA3, OVCA420, OVCA432, OVCA633 and OVCA 810) and Mucinous (MCAS, RMUG-L), and the normal human ovarian surface epithelial (Hose 11 and Hose 17-1) cells have been described previously [17]. These cells were bought from National collection of authenticated cell cultures (Shanghai, China) for research purpose only. HOSE cells were immortalized by an HPV E6/E7 gene introduction for research use purpose. Ovarian cancer cell lines were cultured in a medium mixture of MCDB105 medium and 199 (1:1) (Sigma, St. Louis, MO), and supplemented with 10% fetal calf serum (Invitrogen, Carlsbad, CA) and maintained in a 37 °C humidified atmosphere [95% O_2+ 5% CO_2].

Whole transcriptome expression profiling

RNA was extracted from control and PAFAH1B2 KD cells by TRIzol reagent kit (Invitrogen, Carlsbad, CA). The RNA quality and quantity of samples were tested using spectrophotometric analysis and Bioanalyzer (Agilent Technologies, Santa Clara, CA). RNA was extracted from cell lines using TRIzol reagent (Invitrogen, Carlsbad, CA). 1 ug of RNA per each sample were used for target labelling by a two-round amplification protocol. Expression profiles were determined using 4.5µg of fragmented, labelled and hybridized with per Chip (Human Gene whole transcript 1.1 ST Arrays, Affymetrix) The expression data were normalized by RMA pre-processing protocol, background-corrected, and log2-transformed for parametric analysis. All internal control genes were removed and the remaining probe clusters were imported into the Affymetrix Power Tools software (APT package) for next step analsysi. Differentially expressed genes were identified using significance analysis of microarrays (SAM) with the R package 'samr' (false discovery rate (FDR) <0.05; fold change >2) and determining the gene list based on the number of significant genes that were identified by fold change. Two-dimensional hierarchical clusters are generated.

Metascape pathway Analysis

Gene ontology (GO) and pathway enrichment analysis of PAF-AH IB2 KD - associated significantly changed genes were performed using Metascape (http://metascape.org/)[18]. In this study, an ordered list of genes was first generated by GSEA based on correlation with PAF-AH IB2 KD. The significant

survival difference observed between control and PAF-AH IB2 KD was elucidated. Gene set permutations were performed 1,000 times each analysis. The nominal p-value and normalized enrichment score (NES) were used to classify the pathways enriched in each phenotype.

Tumour tissue array Immunohistochemistry analysis

Ovarian cancer tumour tissue microarray was bought from bioaitech (product ID: F100Ov01, xi'an, China), which contained formalin-fixed, paraffin-embedded normal, benign, and cancerous ovarian tissues with identified pathological diagnosis. The array included specimens of 100 ovarian malignancies of surface epithelial origin that representing 5 different histologic types. Sections (5 mm) were applied to detect expression of PAFAH1B2 in ovarian tumour tissues. Briefly, slides were deparaffinized in xylene and rehydrated by a series of graded alcohols buffers, and then 3 min boiled process in a pressure pot to retrieve the antigens. The 3% hydrogen peroxidase 10 min-treatment was used to block endogenous peroxidases. The sections were incubated with PAFAH1B2 antibody (20365-1-AP, Proteintech, China; overnight, 4°C). The peroxidase conjugated secondary antibody (37 °C, 30 min) was incubated with sections and performed the chromogenic with a DAB Substrate Kit, and then counterstained with hematoxylin. The slides were then dehydrated in graded alcohol buffers and covered with coverslips. Staining intensity and percentage of PAFAH1B2-positive tumour cells were observed by microscope and assessed. The staining tumour tissue images were observed and evaluated by ImageJ software and IHC Profiler plugin[19]. The intensity of slide immunohistochemistry was scored automatically after the slides counting. The IHC scored values are represented as means±SEM. The ANOVA analysis was used to compare the mean values of IHC scores between benign and different tumour histological types.

Lentiviral knockdown and plasmid transfection

The lentiviral PAF-AH Ib2-targeting and non-target control shRNA transduction particles (Mission™) were purchased from Sigma-Aldrich (St. Louis, MO). To generate stable knockdown of PAF-AH IB2, ovarian cancer cells (MCAS, SKOV3, OV432, RMGUL; 1 x 10^5 cells) were growing in complete medium and infected with lentivirus containing pLKO short-hairpin RNA (ShRNA) constructs for PAF-AH IB2 (Sigma). After 48 h infection, cells were screened with medium containing puromycin (2 mg/ml) as the lentivirus vector contained this selection resistance marker for 2 weeks. Stable PAF-AH1b2 knockdown cell lines were validated by Western blot.

Proliferation and scratch wound healing assay

The cell proliferation and cytotoxicity of the drugs to ovarian cancer cells were tested by tetrazolium-based MTT method [20] in time point manners. Briefly, at the beginning, the single cells solution was (5,000 cells /well) allocated into each well of 96 wells. For proliferation assay, the cells were cultured as normal, and MTT dye solution was added to each well (10μl/well) after per 24h cultured to incubate at

37°C for 4 hours in a humidified chamber. For drug toxicity assay, the drugs were added into plate wells after cells were completely attached. After 48 hours of treatment, MTT dye solution was added into and incubated (37°C, 4 hours) in a humidified chamber. After incubation, solubilization/stop solution (100µl/well) was added and incubated for one hour, the content of wells was mixed and read by 96-well plate scanning spectrophotometer (µQuant) and quantitative software (KC-junior, Bio-Tek Instruments, Inc.) (Absorbance value in 630 nm) for quantitative analysis. The scratch wound healing was performed using a 6 well plate. The cells were cultured as for 24h to form a confluent monolayer, then scratches were performed using a 10-µl tip and the culture medium was replaced with fresh complete medium. At the start of experiment, after 12h, 24 h and 48h of incubation, the plates were checked under microscope and took images to track the scratches width. All the images were converted as 8-bit images and analysed using Image J programmer to quantitative calculate the scratches width.

Cell proliferation, invasion/migration in real time by xCELLigence system

The dynamic of cell proliferation, adhesion and migration were assessed by measuring cell amount in real time manner through a xCELLigence system and E plates (Roche). It could monitor cellular events in real time through measuring electrical impedance across interdigitated gold micro-electrodes integrated on the bottom of tissue culture plates. This dynamic measurement provides quantitative data about the biological status of the cells, including cell number, viability and morphology [21]. Briefly, for determination of cell survival and proliferation, E-plate 96 (Roche Applied Science) assemblies were seeded with MCAS/SKOV3 cells (2.0 x 10^4 cells/well). Plate was assembled on the RTCA DP analyzer, and collecting data with 5-min intervals for 20 h (37 °C, 5% CO_2). To examine cell adhesion and migration, serum free medium was added to E-plate 16 to obtain background readings, and cells were added to wells of a CIM plate 16 (Roche Applied Science; 8-µm pore size), and dried the membranes at 25 °C for 1 h. The lower chambers were added with fresh medium (10% FBS or with serum-free medium), whereas the upper chambers were filled with serum-free medium (30µl/well) [37 °C, 5% CO_2, 1 h]. The cells were added to each well and balance for a while [25 °C, 30 min], then assembled the CIM plate onto the RTCA DP analyzer. The cell migration was assessed for 24 h (37 °C, 5% CO_2) with 5-min intervals. The data were analysed using the provided RTCA software. The extent of change is proportional to the cell number, morphological and adhesive features. The more cells that are growing on the electrodes, the higher value of electrode impedance increases [21]. Cell index (CI) slope is defined to represent cell status according to the measured relative change in electrical impedance that occurs in the presence or absence of cells in the wells, which is calculated by the following formula: CI=(Zi–Z0)/15, where Zi represents the impedance at an individual time point during the experiment, and Z0 is the impedance at the start of the experiment [22].

Colony-Forming Assays in agar gel

The scramble control and stable PAF-AH IB2 KD of MCAS Cells were cultured in soft agar gel for additional 30-day cultured followed the protocol. The cancer cells formed colonies were stained (0.5% crystal violet/20% ethanol) and taken image by light microscope. The colonies numbers were calculated by using Image J software.

Western blotting

Cells were washed with cold PBS (phosphate buffered saline) for twice, and the cellular lysates were prepared in ice-precold lysis buffer (10 mM Tris-HCl pH 7.4, 150 mM NaCl, 1 mM Na3VO4, 2 mM EDTA, 2 mM EGTA, 50 mM NaF, 1% NP-40, 1% sodium deoxycholate, 0.1% SDS, 0.5 mM DL-dithiothreitol and proteinase inhibitor cocktails, Pierce), and homogenized using a Sonic Dismembrator 100 (Fisher Scientific Inc., MA). The cell lysates protein concentration was determined by MicroBCA kit (Pierce) and equal amount of total proteins from different cell lysates were resolved by SDS-PAGE (4 ~12%) for Western blotting with antibodies against PAF-AH 1B1/B2/B3, beta-actin, phosphorylated p44/42 (Thr202/Tyr204), phosphorylated Akt (Ser473), phosphorylated p53 (Ser15), phosphorylated p21 Waf1, phosphor-Chk2 (Thr68), phosphorylated-CDC2 (Tyr15) and CDC (Cell Signaling, CA). Primary antibodies were visualized by secondary antibodies of goat-anti mouse (IRDye 680CW) or goat-anti rabbit (IRDye 800CW) through an Odyssey scanner (Li-cor biosciences).

Luminex assay

The total tyrosine kinases profiles of target cells, including 62 of the 90 tyrosine kinases in the human genome, were performed by Luminex xMAP microspheres (Luminex Corporation, Austin, TX) system, which was coupled individual bead-type of antibody to capture target. According to manufacturer's recommended procedure, each bead-type of Luminex xMAP microspheres (100 ul, Luminex Corporation, Austin, TX) were coupled separately to antibodies and performed the assays as previously described [23]. Briefly, test data were acquired through a Luminex FlexMAP 3D instrument (Luminex Corporation). The background readings value for each capture antibody were normalized by microspheres with 1x cell lysis buffer (Cell Signaling Technology). Reading values were defined as positive only that higher threefold over the background. The results were normalized against unstimulated EGFR and presented as a fold change in relative phosphorylation. Final average results were generated from three independent experiments.

Flow cytometry for cell apoptosis analysis

Samples were measured by BrdU-488/PI through flow cytometry (Accuri C6 Biosciences) for cell apoptosis analysis. The cells were stained exactly as recommended by the manufacturer of the Annexin kit (Promega, MA). Briefly, cells (5-10x104) were cultured and labelled in the anoxic treatment groups and the normal oxygen groups in their medium. The cells were washed with PBS, and incubated with serum

free medium for the desired times. Then, the cells were harvested with trypsin solution and washed twice with PBS. BrdU-488/PI were added into the tube and gently mixed with cells in dark condition [room temperature, 10 min]. Stained cells were washed 3 times with cold PBS and fixed with then permeabilized with 0.5% Triton X-100 in PBS [5 minutes, room temperature]. Finally, cells were analysed by using the flow cytometer and collected data for result analysis.

Immunofluorescence analysis

The cells were seeded in a Chamber Slides (Nalge Nunc International) and normally cultured overnight. For the Hose cells were transfected with GFP-plasmid, cells were observed by microscopy after 24hour. Cells were treated with drug (PAF, C-PAF, ET-18) for 24 hours and then washed twice with PBS. FITC-VAD-fmk (CaspACE™ FITC-VAD-FMK in Situ Marker, Promega) was used to test caspases activation in cells, which is a cell-permeant fluorochrome derivative of caspase inhibitor Val-Ala-DL-Asp-fluoromethylketone. Cells were washed twice by PBS and FITC-VAD-fmk (5 mM) was incubated with cells (20 min, room temperature) in the dark. Immediately after FITC-VAD-fmk staining procedure (see above), cell was co-stained with Hoechst 33342 (1 mg/ml, 10 min) for counterstaining of nuclei in the dark. Then, washing twice in PBS, cells were then fixed with 0.5% paraformaldehyde (20 min, RT) in the dark. PBS washed twice and cells were resuspended in Vectashield H-100 mounting medium (Vector Laboratories, Burlingame, CA). Cells were blocked overnight at 4°C with blocking buffer (0.1% Triton X-100, 2% BSA in PBS). The Annexin V staining to detect the cell apoptosis was followed the related protocol. Images were visualized using Zeiss Axiovert 200 inverted fluorescence microscope (40 x oil objectives) equipped with 14-bit ECCD camera and argon and krypton gas excitation asters at 488 and 568 nm. Z-stack acquisition using optimal slice distancing was performed on each microscope image.

Statistical Analysis

Significance of differences for the associations between cytotoxicity and enzyme activity, pathway activation status and metabolite profile will be determined using ANOVA with Prism software (GraphPad Software, Inc. San Diego, CA). Significance of the test was defined (*i.e.* p-value ≤ 0.05).

Results

Characterizing the pathological role of PAFAH1B2 in Ovarian Cancer

PAF-AH IB2 was discovered to be overexpressed in 426 ovarian cancer cases compared to normal ovarian tissue (n=88, Fig.1A) in the Gepia Cancer Genomic database, which incorporates a number of published cancer datasets from TCGA [24], and was identified to be dispersed from stage II to stage IV (Fig.1B). Patients with higher levels of PAFAH1B2 expression had a significantly shorter survival time (PFS,

median survival time: 15.01 months, p=0.0098, Fig.1C). PAF-AH IB2 was significantly overexpressed in four subtypes of ovarian tumor tissues (Fig.1D-E) and in all stage's cases (Fig.1F-G), according to immunohistochemical (IHC) staining in ovarian tumour tissue microarray.

Furthermore, when compared to human normal ovarian epithelium (HOSE II, HOSE 2282), Western blot analysis revealed that PAF-AH IB2 was overexpressed in multiple ovarian cancer cell lines and was partially associated with LIS1 subunits overexpression in MCAS, SKOV3 and RMUGL (Fig.2A), including MCAS, SKOV3, Tov112D, OVCA3, OVCA420, OVCA432, OVCA633, OVCA810 and RMUGL (Fig.2A), as well as a negative signal in RMG1 cell. Interesting, we were unable to detect the expression signal of the homologue subunit (PAF-AH IB3) in the ovarian cancer cells by Western blot, despite a positive signal detected in mouse brain lysate.

PAF-AH 1B2 knockdown impaired the cellular functions of ovarian cancer cell

PAF-AH IB2 wild-type cell lines (Ctrl) and PAF-AH IB2 knockdown cells were effectively transduced using lentivirus harboring control shRNA or PAF-AH IB2 shRNA constructs, resulting in PAF-AH IB2 wild-type cell lines (Ctrl) and PAF-AH IB2 knockdown cells, respectively (Fig. 2B). PAF-AH IB2 knockdown did not result in expression compensation of homologous subunit (PAF-AH IB3) or other component (Lis1) in cancer cells (MCAS and SKOV3) (Fig. 2B). The knockdown cell lines showed a significantly decreased in ability of colonies forming in vitro soft agar (Fig 2C, $p<0.001$) and a significantly slower rate of proliferation (Fig 2D), as well as a decrease in cell migratory capabilities, as compared to the control cell lines (Fig.2E, MCAS). Furthermore, we used the xCELLigence system to get the dynamic information about proliferation and investigate whether knockdown would affect the proliferation and migratory abilities of ovarian cancer cells (MCAS, SKOV3). PAF-AH 1B2 knockdown cells showed significant slower proliferation rate than control's (Fig.2F, $p<0.001$). The knockdown of PAF-AH 1B2 consistently reduced the migration ability in ovarian cancer cell (Fig. 2G).

Growth inhibition of non-hydrolysable PAF analogues on ovarian cancer cells

PAF-like ether lipid analogues with non-hydrolyzable sn-2 side chains were found to have tumor cell-directed cytotoxicity in vitro [25, 26]. To investigate the efficacy of PAF and its non-hydrolysable analogues in causing tumor cell cytotoxicity, we treated ovarian cancer cell lines with various doses of PAF and two non-hydrolysable analogues: C-PAF (an N-methylcarbamyl moiety at the sn2 position) and edelfosine (a methyl ether linkage at the sn2 position, Sup Fig.1A) and calculated the IC_{50} value in each cancer cell, respectively. PAF exhibited mild cytotoxicity on ovarian cancer cells (MCAS, TOV112D, RMGUAL, SKOV3 and OVCA3) and had no cytotoxic effect on RMG1 (Sup Fig.1B-G). It is concluded that higher levels of PAF-AH IB2 expression in these cancer cells would cause PAF to be digested more quickly

(Fig.2A). C-PAF or edelfosine treatment, on the other hand, demonstrated significant cytotoxicity on these ovarian cancer cells (Sup Fig. 1B &G).

Transcriptome analysis discovered key functions and Pathways Regulated by PAFAH1B2 in ovarian cancer cell

The whole transcriptome profile analysis was used to identify the significantly regulated functions and key pathways that PAF-AH 1B2 KD regulates in ovarian cancer cells. Through data normalization and significantly analysis filtering (Fold change >2.0 or <-2.0, P< 0.001), 826 genes (up-regulated 7 genes; down-regulated 819 genes, Table.S1) were identified as significantly changed and computationally clustered in the PAFAH1B2 KD vs control of MCAS cancer cells (Table.S1, Fig.3A). To identify the role and regulatory mechanism of PAFAH1B2 in ovarian cancer, the significant changed genes were blast through Metascape to enrich the key GO processes and pathways that regulated by the PAFAH1B2 KD. The top twenty enriched functional pathways that are significantly regulated have been summarized (Table.S2, Fig.3B), which were chosen from three categories: GO biological process (BP), pathways and Reactome gene sets. The enriched representative GO functions included Translation (GO:0006412), endomembrane system organization (GO:0010256), response to endoplasmic reticulum stress (GO:0034976), neutrophil degranulation (GO:0043312), cellular protein catabolic process (GO:0044257), regulation of binding (GO:0051098), apoptotic signaling pathway (GO:0097190) and supramolecular fibre organization (GO:0097435) were among the representative enriched GO functions. The VEGFA-VEGFR2 signaling pathway and apoptosis signaling pathway were listed in the top 10 enriched pathways (Table.S2). Furthermore, the interaction pathways identified the key functional network controlled by PAFAH1B2 (Fig.3C).

According to these results, it is suggested that PAFAH1B2 play important regulatory roles in abnormally cell proliferation and adhesion in ovarian cancer cells. The apoptotic signaling pathway and VEGFA-VEGFR2 signaling pathway, in particular, had been highlighted in the enrichment pathways of PAFAH1B2 KD cancer cells and had been chosen for next step analysis.

PAF-AH IB2 knockdown causes caspases activation and G2-M cell cycle arrest

Flow cytometric analysis revealed that PAF-AH IB2 knockdown caused cell cycle arrest in ovarian cancer cells (Fig.4A). The percentages of cell cycle G2/M phase of PAF-AH IB2 knockdown cells were significantly increased when compared to controls, respectively (Fig.4B, ** p<0.01). In addition, PAF-AH IB2 knockdown cells induced more positive Annexin V signal and caused the cells more sensitive to PAF than control cells, and while the c-PAF treatment did not demonstrate this difference (Fig.4C&D). Through the western blot analysis, the phosphorylation levels of several key regulatory proteins, including p53-Ser15, Akt-Ser473, CDC2-Tyr15, Chk2-Tyr68, and p21Waf1 and CDC2 that are associated with cell growth

and cell cycle arrest regulation [27]·[28, 29]·[30], were significantly increased in PAF-AH 1B2 KD MCAS cells (Fig.4E), while the phosphorylation of p44/42 MAPK was decreased, which was used as a molecular indicator of tumour cell proliferation and growth. The phosphorylation of Akt-Ser473 was significantly reduced in p53-deficient PAF-AH 1B2 knockdown SKOV3 cells. Together, it is suggested that the p44/42–Akt–Mdm2-p53 pathway is the downstream signalling of PAF-AH IB2 and is responsible for the cell proliferation inhibition in knockdown ovarian cancer cells.

Furthermore, when compared to controls, PAF-AH 1B2 KD significantly increased PAF's growth inhibitory effect and shifted the dose curve in ovarian cancer cells (Sup Fig.2A), whereas the cytotoxicity of two non-hydrolyzable analogues, C-PAF and edelfosine (ET-18), on PAF-AH IB2 knockdown and control cells was not significantly different (Sup Fig.2B&C). In PAF-AH IB2 knockdown cells, the percentages of positive caspases caspase activated (substrates VAD-FMK) per cells were considerably higher under rest condition and treated with PAF compared to controls (Sup Fig.2D, ** $p<0.01$). When PAF-AH IB2 KD cells were treated with C-PAF and edelfosine, the positive signaling of caspase activation staining did not differ substantially from control cells. According to western blot analysis, PAF and C-PAF treatment did not induce compensated expression of PAFAH1B3 in PAFAH1B2 KD or control cells (Sup Fig.2F). In PAFAH1B2 KD cells, PAF treatment reduced phosphorylation of p44/42 MAPK, whereas C-PAF treatment greatly boosted it. When compared to the control cells, the FAK was upregulated in the PAFAH1B2 KD during rest and PAF treatment, whereas C-PAF treatment did not show difference. These results imply that overexpression of PAH-AH 1B2 in ovarian cancer cells play a critical role in digesting intracellular PAF and reducing the caspases activation and apoptosis triggered by PAF.

Over-expression of the catalytic subunits in human ovarian surface epithelium induces apoptosis

Transient over-expression studies on normal HOSE cells were conducted to gain a better understanding of the cellular function of the PAFAH1B2. Initially, GFP conjugated transient over-expression of human PAFAH1B2 WT caused considerable cellular toxicity, resulting in HOSE phenotypic alterations and sickness after 48-hour transfection, as well as rapid death (Fig.5A), but pEGFP-C1 vector transfected cells grew normally. It is 100% identified rate of human and mouse PAFAH1B2 wild type (WT) protein sequences (Fig.5B). The mice PAFAH1B2 WT or functional mutants (E39D, S48C) were transfected with the Lis1 (human) unit into cells, and caspase activation by FITC-VAD-FMK was detected in living cells. The activation of caspases was induced by transfection of mouse PAFAH1B2 WT with Lis1 or functional mutants (E39D) (Fig.5C). Positive caspase activation signals were eliminated when cells were transfected with an enzymatic mutant (S48C) or a dual mutant (E39D, S48C). Furthermore, endogenous caspase 8 was activated by western blot in HOSE transfected with mouse PAFAH1B2 WT and mutants (E39D), whereas caspase 8 activation was inhibited by mouse PAFAH1B2 mutants (S48C) or (E39D, S48C). The activation of caspase 8 was validated using a cleaved Caspase-8 (Asp374) antibody, which specifically detects endogenous cleavage at aspartic acid 374 by western blot (Fig.5D). The downstream effector caspases, such as caspase-1, -3, -6, and -7, will be activated after caspase 8 activation. Caspase-3

ultimately elicits the morphological hallmarks of apoptosis, including DNA fragmentation and cell shrinkage [31]. Thus, over-expression of PAFAH1B2 resulted in caspase 8 activation and HOSE death.

PAFAH1B2 knockdown caused the down regulated aberrant-activation of multiple tyrosine kinases signalling pathways in ovarian cancer cell

As the VEGFA-VEGFR2 signaling pathway, had been highlighted in the enrichment pathways of PAFAH1B2 KD cancer cells, exploring the related significantly changed genes via the WikiCancer network, the signaling pathway network and significantly changed genes were visualized (Fig.6A), which contained several tyrosine kinases and downstream signalling pathways, like MAPK and PI3K/AKT to regulate cell proliferation and growth. Upward thermometers are red and indicate up-regulated signals, while downward thermometers are green and indicate down-regulated gene expression levels. The majority of the involved genes, such as FGFR1, GRB2, ERBB2, and MAPK1, were down-regulated.

To explore the impact of PAF-AH 1B2 KD on the profiling tyrosine kinase activation, we tested the aberrant tyrosine kinase activity. Using a Luminex assay, we also tested the phosphorylation status of EGFR, ERBB2, GRB2, and SRC, and found that phosphorylation of these proteins was significantly reduced in the PAF-AH 1B2 KD (Fig.6B). These findings support previous findings that tyrosine phosphorylation mediates the association of signaling proteins with EGFR. Furthermore, using western blot analysis, the phosphorating levels of ERBB2 (Tyr1221/1222) and EGFR (Tyr1068) were decreased in PAF-AH 1B2 KD cells, while SRC was increased (Fig.6C). It is suggested that PAFAH1B2 work as the essential signaling mediators of oncogenic multiple tyrosine kinases mediated the cellular transformation as it is abnormally overexpressed in ovarian cancer and promotes proliferation.

Discussion

In this study, PAFAH1B2 was identified as a novel potential biomarker that is important in driving aggressive and tumorigenic features of ovarian cancer through exploring TCGA database, which degrades PAF intracellularly to maintain key reproduction function in ovarian cancer [12]. The overexpression pattern of PAF-AH 1B2 was confirmed in clinic ovarian cancer tissues using immunohistochemical (IHC) staining with ovarian cancer tissue microarray (Fig.1C&D). The protein expression level of PAF-AH 1B2, compared with normal ovarian tissue, was significantly higher in ovarian cancer samples that identified by IHC. However, the expression of a1 subunit did not detect in the tumor tissues (data not show). The abnormally upregulated pattern of a2 was confirmed in the majority of ovarian cancer cell lines by Western blot, compared with normal human ovarian surface epithelium (Fig.2A). These findings suggest that there is an unmask dysregulation network involved in the overexpression of PAF-AH 1B2 in ovarian cancer and normal ovarian physiologic function.

Lipid metabolism, which provides energy and nutrients as well as signalling for tumor survival, growth, and metastasis, has specific implications in signalling for tumour survival, growth, and metastasis[32]. Many lipid metabolites, like lysophosphatidic acid (LPA) and platelet-activating factor (PAF), are bioactive lipids that work as the second messengers to initiate signalling cascades for ovarian tumorigenesis and metastasis [33, 34]. Platelet-activating factor (PAF) is a phospholipid that involved in the inflammation, migration and cell invasion [35, 36]. PAF synthesis, transport, and enzymatic degradation are all tightly regulated and linked to a variety of physiologic processes [36]. The PAF-AH 1B2 enzyme is primarily responsible for PAF intracellular degradation. Extracellular PAF can also be internalized via PAF receptor-independent mechanisms, resulting in caspase-3-dependent apoptosis. The apoptogenic concentration of extracellular PAF could influence PAF-AH 1B2 expression and limit the duration of pathological cytosolic PAF accumulation [37]. In this study, PAF had a minimal growth inhibitive effect on several ovarian cancer cells even at a relatively high concentration (5 mM), whereas the cytotoxic effects of c-PAF and Edelfosine, which are PAF-like non-hydrolysable ether lipid analogues that selectively kill tumor cells while sparing normal cells, were quite strong at the same concentration [38]. It was suggested that ovarian cancer cell lines have high intracellular enzymic activity to counteract the cytotoxic effect of PAF.

Abnormal expression of PAF-AH1B2 will cause the physiologic function defect. Knockout α2 resulted in sterile and defective spermatogenesis in mice as well as a reduction in Lis1 protein expression [39, 40]. The abilities of PAF-AH 1B2 knockdown cancer cell to proliferate, migrate (Fig.2D), and forming colonies in vitro soft agar (Fig.2C) was significantly reduced. Because the expression pattern of the other subunits, particularly a1 (PAFAH1B3), remains unchanged, it suggests that abnormal enzymatic activity of PAF-AH 1B2 plays a dominant role in ovarian cancer. Furthermore, knocking out PAF-AH 1B2 significantly increased PAF's cytotoxic effect on cancer cells (**Sup Fig. 2A**). It corresponds to the intracellular counterbalancing role of PAF-AH 1B2. These findings imply that PAF-AH 1B2 has the potential to be a synergistic chemotherapy target for ovarian cancer.

Furthermore, knockdown PAF-AH 1B2 caused caspases activation and cancer cells cycle arrest, apoptosis, as well as significant rise the phosphorylation levels of related regulatory proteins p53-Ser15, Akt-Ser473, CDC2-Tyr15, Chk2-Tyr68, and the protein level of p21Waf1 and CDC2 (Fig.4E), which are associated with relate regulation [28, 29]. A recent study found that LPA can induce $p21^{Waf1}$ expression and mediate cytostatic response in cancer cells [41], which is consistent with our findings. Combined previously results, it hints that there is a novel regulation network that knockdown of PAF-AH IB2 might cause a feedback loop for the increased biosynthesis of MAGE and LPA. LPA exhibits pleiotropic biological functions, depending on which G protein-coupled receptors (GPCR) it interacts with [42, 43].

It is well established that α2 has a stronger affinity for LIS1 than does α1 subunit [40]. PAFAH1B2 could form homodimer, and the position of Glu39 is critical for binding with Lis1 and Ser47 is key site of the catalytic centre [15, 40]. To explore the mechanism of PAFAH1B2 abnormal expression in HOSE cells to determine whether this enzyme was sufficient to confer oncogenic properties, both the catalytically active and the inactive mutant form of PAFAH1B2 (E39D, S48C, E39D/S48C), with or without Lis1, were transiently overexpressed in HOSE, respectively. While overexpression of the wild- type form of PAFAH1B2

activated caspases, endogenous caspase 8 was cleaved and HOSE died soon (Fig.5A, C&D). The catalytically inactive mutant (S48C, E39D/S48C) totally reversed these positive activation and phenotype changes. Since PAFAH 1B2 has been shown to interact with PAFAH1B1, LIS1, our results also indicated that even co-overexpression Lis1 with PAFAH1B2 WT may be not sufficient to induce the abnormally proliferation in the HOSE, hinting missed a link between over-expression of the PAFAH1B2 and ovarian cancer genesis. It is strongly suggested that some newly discovered materials, when combined with PAFAH1B2 overexpression, can transform normal HOSE into malignant features of cancer. Furthermore, the Luminex assay and western blot results demonstrated that the phosphorylation level of EGFR, ERBB2, GRB2, and SRC were significantly reduced in the PAF-AH 1B2 KD cancer cells (Fig.6B). These results support previous findings that PAF-PAFR signaling pathway could synergistically be activated with tyrosine kinase -VEGFR pathway to modulate the abnormal proliferation in ovarian cancer [44, 45]. It is strongly suggested that PAFAH1B2 act as the essential signaling mediator of oncogenic tyrosine kinases signalling pathways mediated cellular transformation as it is abnormally overexpressed in ovarian cancer and promotes proliferation.

Conclusion

In conclusion, our results shed new light on the role of the PAF-AH IB2 and regulated pathways in ovarian pathogenesis, leading to the identification of new marker and signalling for ovarian cancer, as well as new potential preventive and therapeutic strategies to target the enzyme. Together, our findings and those of others show a novel interaction network of lipid metabolic PAF-AH 1B2 and other enzymes in ovarian cancer. Future research will concentrate on elucidating signal transduction from ether lipid messengers to downstream pathways in order to better understand how PAFAH1B2 regulates the metabolic and signalling pathways in ovarian pathogenesis. Another direction will also focus on the regulation mechanism of PAF-AH 1B2 abnormal expression in ovarian cancer.

Declarations

Acknowledgements

Not applicable.

Funding

This work was supported by start-up program (Y8677211K1, Y8690211Z1, E0241211H1) from State Key Laboratory of Phytochemistry and Plant Resources in West China, Kunming Institute of Botany, Chinese Academy of Sciences to Dr. Shubai Liu. These grants were mainly used to support the research activities of this project, including experiments and data collection, analysis and interpretation, manuscript preparing and publication cost.

Author information

Affiliations

State Key Laboratory of Phytochemistry and Plant Resources in West China, Kunming Institute of Botany, Chinese Academy of Sciences, Kunming, 650201 Yunnan, P. R. China.

Yingying He, Zhicheng He, Xiaoyu Zhang, Shubai Liu

School of Chemical Science & Technology, Yunnan University, Kunming, Yunnan 650091, China;

Yingying He.

University of Chinese Academy of Sciences, Beijing 100049, China.

Zhicheng He, Shubai Liu.

Contributions

YH and SL had designed the study plan of project; YZC, XYX, YH and SL did experiments, collected data, performed data analysis; SL, YH summarized the results; YH and SL wrote and revised the manuscript; all authors had read and approved the final version of manuscript.

Ethics approval and consent to participate

Not applicable.

Consent for publication

Not applicable.

Competing interest

Not applicable.

References

1. Altekruse S, Kosary C, Krapcho M, Neyman N, Aminou R, Waldron W, Ruhl J, Howlader N, Tatalovich Z, Cho H*et al*: **SEER Cancer Statistics Review, 1975-2007**. In.: National Cancer Institue. Bethesda, MD, USA; 2010.

2. Fukami T, Yokoi T: **The emerging role of human esterases**. *Drug Metab Pharmacokinet*2012, **27**(5):466-477.
3. Kohnz RA, Mulvihill MM, Chang JW, Hsu KL, Sorrentino A, Cravatt BF, Bandyopadhyay S, Goga A, Nomura DK: **Activity-Based Protein Profiling of Oncogene-Driven Changes in Metabolism Reveals Broad Dysregulation of PAFAH1B2 and 1B3 in Cancer**. *ACS Chem Biol*2015, **10**(7):1624-1630.
4. McGoldrick CA, Jiang YL, Paromov V, Brannon M, Krishnan K, Stone WL: **Identification of oxidized protein hydrolase as a potential prodrug target in prostate cancer**. *BMC Cancer*2014, **14**:77.
5. Ryan JP, Spinks NR, O'Neill C, Wales RG: **Implantation potential and fetal viability of mouse embryos cultured in media supplemented with platelet-activating factor**. *J Reprod Fertil*1990, **89**(1):309-315.
6. Roudebush WE, Minhas BS, Ricker DD, Palmer TV, Dodson MG: **Platelet activating factor enhances in vitro fertilization of rabbit oocytes**. *Am J Obstet Gynecol*1990, **163**(5 Pt 1):1670-1673.
7. Chen J, Yang L, Foulks JM, Weyrich AS, Marathe GK, McIntyre TM: **Intracellular PAF catabolism by PAF acetylhydrolase counteracts continual PAF synthesis**. *J Lipid Res*2007, **48**(11):2365-2376.
8. Arai H: **Platelet-activating factor acetylhydrolase**. *Prostaglandins Other Lipid Mediat*2002, **68-69**:83-94.
9. Tjoelker LW, Stafforini DM: **Platelet-activating factor acetylhydrolases in health and disease**. *Biochim Biophys Acta*2000, **1488**(1-2):102-123.
10. Hattori M, Adachi H, Tsujimoto M, Arai H, Inoue K: **The catalytic subunit of bovine brain platelet-activating factor acetylhydrolase is a novel type of serine esterase**. *J Biol Chem*1994, **269**(37):23150-23155.
11. Adachi H, Tsujimoto M, Hattori M, Arai H, Inoue K: **cDNA cloning of human cytosolic platelet-activating factor acetylhydrolase gamma-subunit and its mRNA expression in human tissues**. *Biochem Biophys Res Commun*1995, **214**(1):180-187.
12. Yasuda K, Okumura T, Okada H, Nakajima T, Aoki J, Arai H, Inoue K, Nishizawa M, Ito S, Kanzaki H: **Platelet-activating factor acetylhydrolase isoforms I and II in human uterus. Comparisons with pregnant uterus and myoma**. *Biol Reprod*2001, **64**(1):339-344.
13. Kobayashi F, Sagawa N, Ihara Y, Kitagawa K, Yano J, Mori T: **Platelet-activating factor-acetylhydrolase activity in maternal and umbilical venous plasma obtained from normotensive and hypertensive pregnancies**. *Obstet Gynecol*1994, **84**(3):360-364.
14. Maki N, Magness RR, Miyaura S, Gant NF, Johnston JM: **Platelet-activating factor-acetylhydrolase activity in normotensive and hypertensive pregnancies**. *Am J Obstet Gynecol*1993, **168**(1 Pt 1):50-54.
15. Zhang J, Zhuang L, Lee Y, Abenza JF, Penalva MA, Xiang X: **The microtubule plus-end localization of Aspergillus dynein is important for dynein-early-endosome interaction but not for dynein ATPase activation**. *J Cell Sci*2010, **123**(Pt 20):3596-3604.
16. Tang Z, Li C, Kang B, Gao G, Li C, Zhang Z: **GEPIA: a web server for cancer and normal gene expression profiling and interactive analyses**. *Nucleic Acids Res*2017, **45**(W1):W98-W102.

17. Huang KC, Park DC, Ng SK, Lee JY, Ni X, Ng WC, Bandera CA, Welch WR, Berkowitz RS, Mok SC*et al*: **Selenium binding protein 1 in ovarian cancer**. *Int J Cancer*2006, **118**(10):2433-2440.
18. Zhou Y, Zhou B, Pache L, Chang M, Khodabakhshi AH, Tanaseichuk O, Benner C, Chanda SK: **Metascape provides a biologist-oriented resource for the analysis of systems-level datasets**. *Nat Commun*2019, **10**(1):1523.
19. Varghese F, Bukhari AB, Malhotra R, De A: **IHC Profiler: an open source plugin for the quantitative evaluation and automated scoring of immunohistochemistry images of human tissue samples**. *PLoS One*2014, **9**(5):e96801.
20. Alley MC, Scudiero DA, Monks A, Hursey ML, Czerwinski MJ, Fine DL, Abbott BJ, Mayo JG, Shoemaker RH, Boyd MR: **Feasibility of drug screening with panels of human tumor cell lines using a microculture tetrazolium assay**. *Cancer Res*1988, **48**(3):589-601.
21. Xing JZ, Zhu L, Jackson JA, Gabos S, Sun XJ, Wang XB, Xu X: **Dynamic monitoring of cytotoxicity on microelectronic sensors**. *Chem Res Toxicol*2005, **18**(2):154-161.
22. GmbH RD: **Introduction of the RTCA SP Instrument. RTCA SP Instrument Operator's Manual**. *A Acea Biosciences Inc*2008:14-16.
23. Du J, Bernasconi P, Clauser KR, Mani DR, Finn SP, Beroukhim R, Burns M, Julian B, Peng XP, Hieronymus H*et al*: **Bead-based profiling of tyrosine kinase phosphorylation identifies SRC as a potential target for glioblastoma therapy**. *Nat Biotechnol*2009, **27**(1):77-83.
24. Cerami E, Gao J, Dogrusoz U, Gross BE, Sumer SO, Aksoy BA, Jacobsen A, Byrne CJ, Heuer ML, Larsson E*et al*: **The cBio cancer genomics portal: an open platform for exploring multidimensional cancer genomics data**. *Cancer Discov*2012, **2**(5):401-404.
25. Mollinedo F, Gajate C, Martin-Santamaria S, Gago F: **ET-18-OCH3 (edelfosine): a selective antitumour lipid targeting apoptosis through intracellular activation of Fas/CD95 death receptor**. *Curr Med Chem*2004, **11**(24):3163-3184.
26. van Blitterswijk WJ, Verheij M: **Anticancer alkylphospholipids: mechanisms of action, cellular sensitivity and resistance, and clinical prospects**. *Curr Pharm Des*2008, **14**(21):2061-2074.
27. Bobrovnikova-Marjon E, Grigoriadou C, Pytel D, Zhang F, Ye J, Koumenis C, Cavener D, Diehl JA: **PERK promotes cancer cell proliferation and tumor growth by limiting oxidative DNA damage**. *Oncogene*2010, **29**(27):3881-3895.
28. Taylor WR, Stark GR: **Regulation of the G2/M transition by p53**. *Oncogene*2001, **20**(15):1803-1815.
29. Rogulski K, Li Y, Rothermund K, Pu L, Watkins S, Yi F, Prochownik EV: **Onzin, a c-Myc-repressed target, promotes survival and transformation by modulating the Akt-Mdm2-p53 pathway**. *Oncogene*2005, **24**(51):7524-7541.
30. Yaginuma Y, Westphal H: **Abnormal structure and expression of the p53 gene in human ovarian carcinoma cell lines**. *Cancer Res*1992, **52**(15):4196-4199.
31. Fernandes-Alnemri T, Armstrong RC, Krebs J, Srinivasula SM, Wang L, Bullrich F, Fritz LC, Trapani JA, Tomaselli KJ, Litwack G*et al*: **In vitro activation of CPP32 and Mch3 by Mch4, a novel human**

apoptotic cysteine protease containing two FADD-like domains. *Proc Natl Acad Sci U S A*1996, **93**(15):7464-7469.

32. Magee T, Seabra MC: **Fatty acylation and prenylation of proteins: what's hot in fat**. *Curr Opin Cell Biol*2005, **17**(2):190-196.
33. Hu YL, Albanese C, Pestell RG, Jaffe RB: **Dual mechanisms for lysophosphatidic acid stimulation of human ovarian carcinoma cells**. *J Natl Cancer Inst*2003, **95**(10):733-740.
34. Bian D, Su S, Mahanivong C, Cheng RK, Han Q, Pan ZK, Sun P, Huang S: **Lysophosphatidic Acid Stimulates Ovarian Cancer Cell Migration via a Ras-MEK Kinase 1 Pathway**. *Cancer Res*2004, **64**(12):4209-4217.
35. Arai H, Koizumi H, Aoki J, Inoue K: **Platelet-activating factor acetylhydrolase (PAF-AH)**. *J Biochem*2002, **131**(5):635-640.
36. Prescott SM, Zimmerman GA, Stafforini DM, McIntyre TM: **Platelet-activating factor and related lipid mediators**. *Annu Rev Biochem*2000, **69**:419-445.
37. Bonin F, Ryan SD, Migahed L, Mo F, Lallier J, Franks DJ, Arai H, Bennett SA: **Anti-apoptotic actions of the platelet-activating factor acetylhydrolase I alpha2 catalytic subunit**. *J Biol Chem*2004, **279**(50):52425-52436.
38. Melnikova V, Bar-Eli M: **Inflammation and melanoma growth and metastasis: the role of platelet-activating factor (PAF) and its receptor**. *Cancer Metastasis Rev*2007, **26**(3-4):359-371.
39. Yan W, Assadi AH, Wynshaw-Boris A, Eichele G, Matzuk MM, Clark GD: **Previously uncharacterized roles of platelet-activating factor acetylhydrolase 1b complex in mouse spermatogenesis**. *Proc Natl Acad Sci U S A*2003, **100**(12):7189-7194.
40. Koizumi H, Yamaguchi N, Hattori M, Ishikawa TO, Aoki J, Taketo MM, Inoue K, Arai H: **Targeted disruption of intracellular type I platelet activating factor-acetylhydrolase catalytic subunits causes severe impairment in spermatogenesis**. *J Biol Chem*2003, **278**(14):12489-12494.
41. Wu J, Mukherjee A, Lebman DA, Fang X: **Lysophosphatidic acid-induced p21Waf1 expression mediates the cytostatic response of breast and ovarian cancer cells to transforming growth factor beta**. *Mol Cancer Res*2011.
42. Mills GB, Moolenaar WH: **The emerging role of lysophosphatidic acid in cancer**. *Nat Rev Cancer*2003, **3**(8):582-591.
43. Ye X, Chun J: **Lysophosphatidic acid (LPA) signaling in vertebrate reproduction**. *Trends Endocrinol Metab*2010, **21**(1):17-24.
44. Aponte M, Jiang W, Lakkis M, Li MJ, Edwards D, Albitar L, Vitonis A, Mok SC, Cramer DW, Ye B: **Activation of platelet-activating factor receptor and pleiotropic effects on tyrosine phospho-EGFR/Src/FAK/paxillin in ovarian cancer**. *Cancer Res*2008, **68**(14):5839-5848.
45. Yu Y, Zhang M, Zhang X, Cai Q, Zhu Z, Jiang W, Xu C: **Transactivation of epidermal growth factor receptor through platelet-activating factor/receptor in ovarian cancer cells**. *J Exp Clin Cancer Res*2014, **33**:85.

Figures

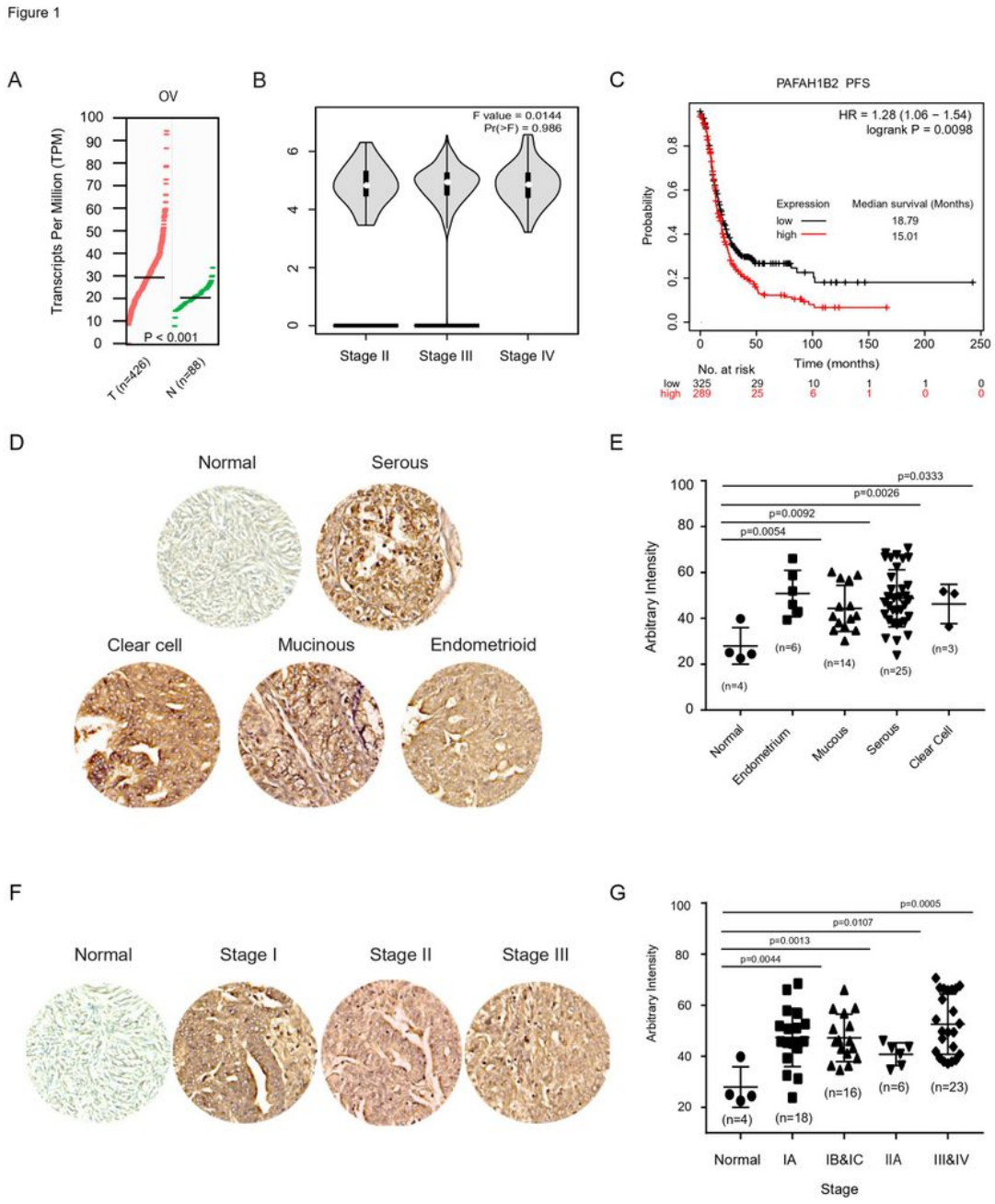

Figure 1

The expression comparison and clinical significance of PAFAH1B2 in ovarian cancer tissues. The expression pattern of PAFAH1B2 in ovarian tumor and NT (normal tissue) are shown Wilcoxon signed ranks test (A) and stage plot (B), including 426 tumor tissues (TCGA) and 88 normal tissues (GTEx). The

comparison of the expression level for PAFAH1B2 mRNA were performed. The log2 (TPM+1) for log-scale was analyzed for stage plot. PFS (P = 0.0098, C) of ovarian cancer patients in was significantly positively associated with the expression of PAFAH1B2. *P < 0.05. Scale bars, 100 mm. Representative images are shown the expression of PAFAH1B2 in normal tissues, various types (D) and stages (F) of ovarian tumor. The IHC staining scores were statistic analyzed between normal and tumor tissues (E&G).

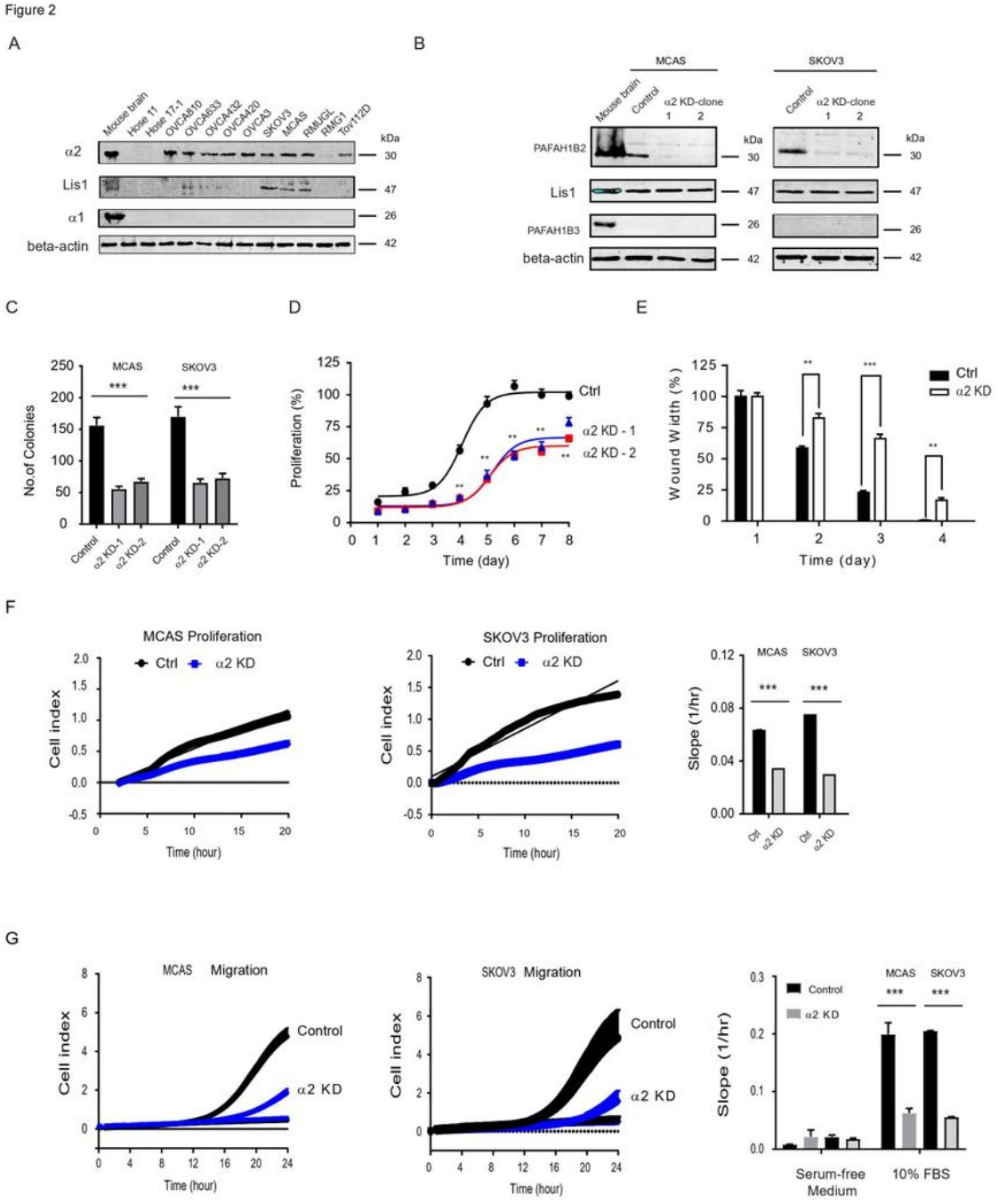

Figure 2

The PAF-AH1B2 mediated the abnormal proliferation and migration in ovarian cancer cell. Ccompared the expression of PAF-AH IB2 subunits in ovarian cancer cell lines lysate by Western blot (A). Validated the PAF-AH 1B2 stable knockdown effect in the ovarian cancer cells by Western blot (B). The comparisons were performed between PAF-AH IB2 and control in the clonogenicity in soft agar (C), cell proliferation in 7 days (D), wound healing migration (E). For the dynamic proliferation test, cells (MCAS, SKOV3, 2.0 x 104 cells/well) were planted by duplicate in the indicated ECM-coated E plates; a non-coated well was used as a negative control (F). Cell proliferation curves were monitored through the xCELLigence system (left panel). The rates of cell proliferation over 24 h (slope) were monitored using the RTCA software (right panel). For dynamic migration assay, cells (MCAS, SKOV3, 2.0 x 104 cells/well) were planted by duplicate in the upper chambers of CIM plates, and the lower chambers were contained with 10% FBS (G). The migration curves were monitored through the xCELLigence system (left panel) and the migration rates over 24 h (Slope) were processed using the RTCA software (right panel). A representative experimental result was generated from three independent experiments. ** $P < 0.01$ and *** $P < 0.001$ as compared to control cells expressing a scramble shRNA control, paired t test.

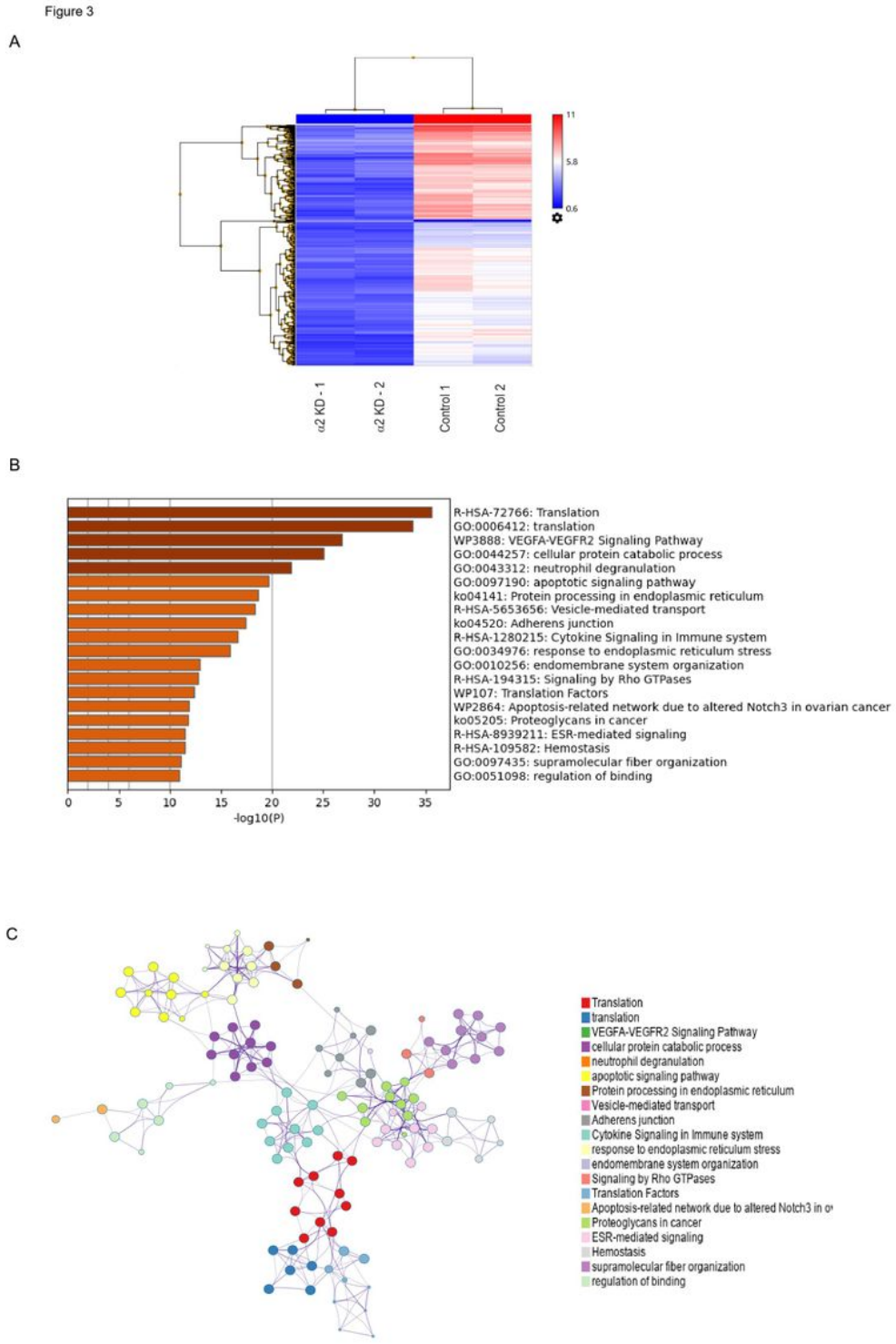

Figure 3

Functional and pathway enrichment analysis of the PAF-AH1B2 knockdown expression profiling in ovarian cancer cells. Heat map demonstrated the significantly changed genes hierarchical cluster analysis of PAF-AH1B2 knockdown transcription profiles in MCAS ovarian cancer cells. The significant changed genes were screened and identified of PAF-AH1B2 vs control (A). Representative Molecular clusters were enriched. Left panel, heatmap of the top 20 enriched terms (B). Representative Molecular

Complex Detection (MCODE) network node demonstrated the connection of significantly changed genes regulated by PAF-AH1B2 knockdown (C). Metascape analysis revealed a Network of enriched sets coloured by ID. Threshold value: 0.3 kappa score; similarity score > 0.3. b Heatmap coloured arranged by P-values.

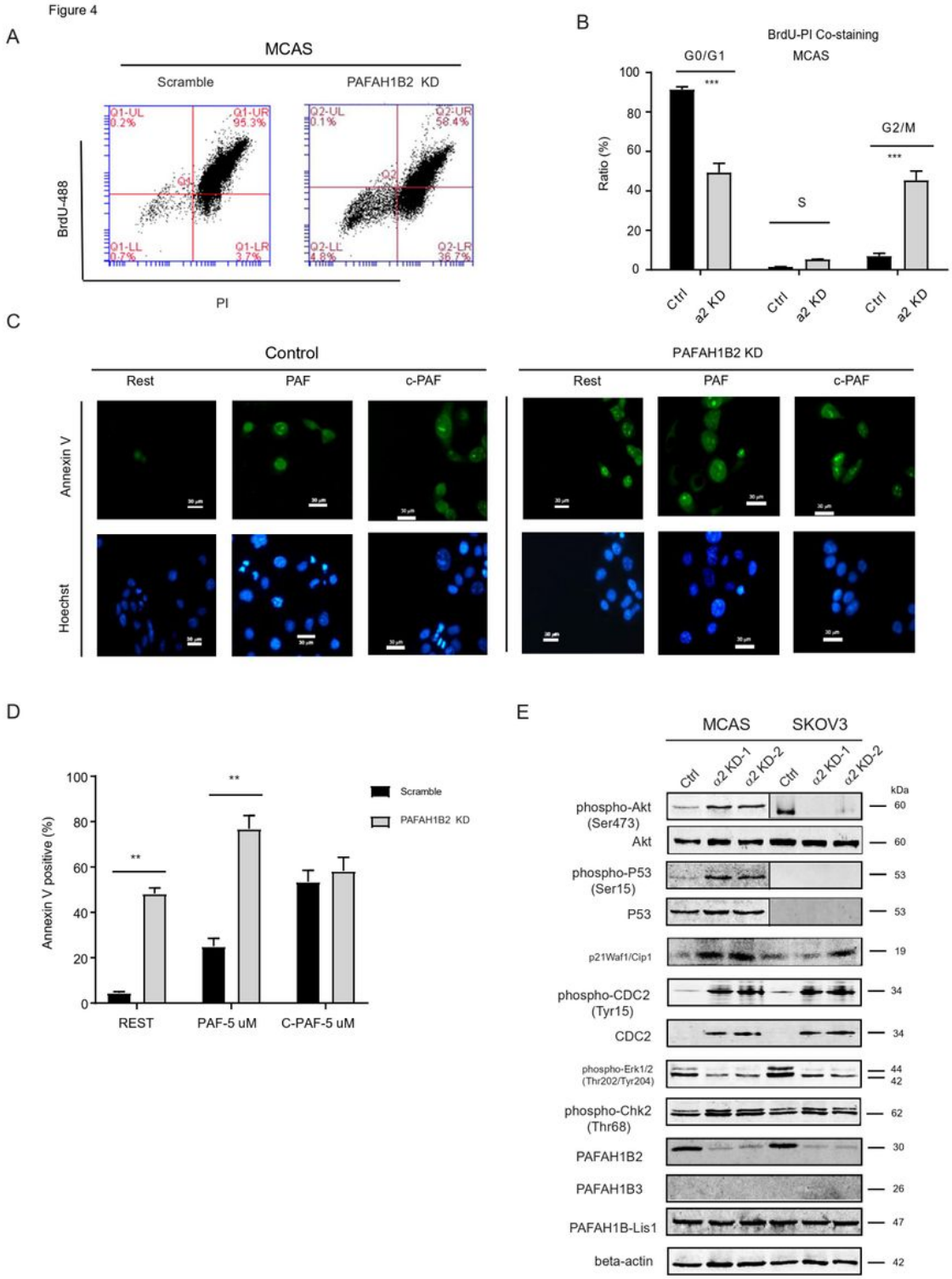

Figure 4

The PAF-AH IB2 KD activated caspases and cell cycle arrest in the ovarian cancer cell. Knockdown PAF-AH 1B2 causes cell cycle arrest of cancer cells identified by BrdU-PI staining analysis (A). Representative histograms for cell cycle phase distribution in control and PAF-AH 1B2 KD cells are shown (B). Using ANNEXIN V (FITC, green) staining kit by fluorene microscope to evaluate the apoptosis effect induced by PAF-AH 1B2 KD and PAF, C-PAF (C & D). Data represent as the mean ± S.E.M (n = 10). Western blot detected the signaling molecules change pattern in the PAF-AH 1B2 KD cells that involved in the cell cycle related signaling pathway (E). * $P < 0.05$ and ** $P < 0.01$ as compared with control cells expressing a scramble shRNA control, paired t test.

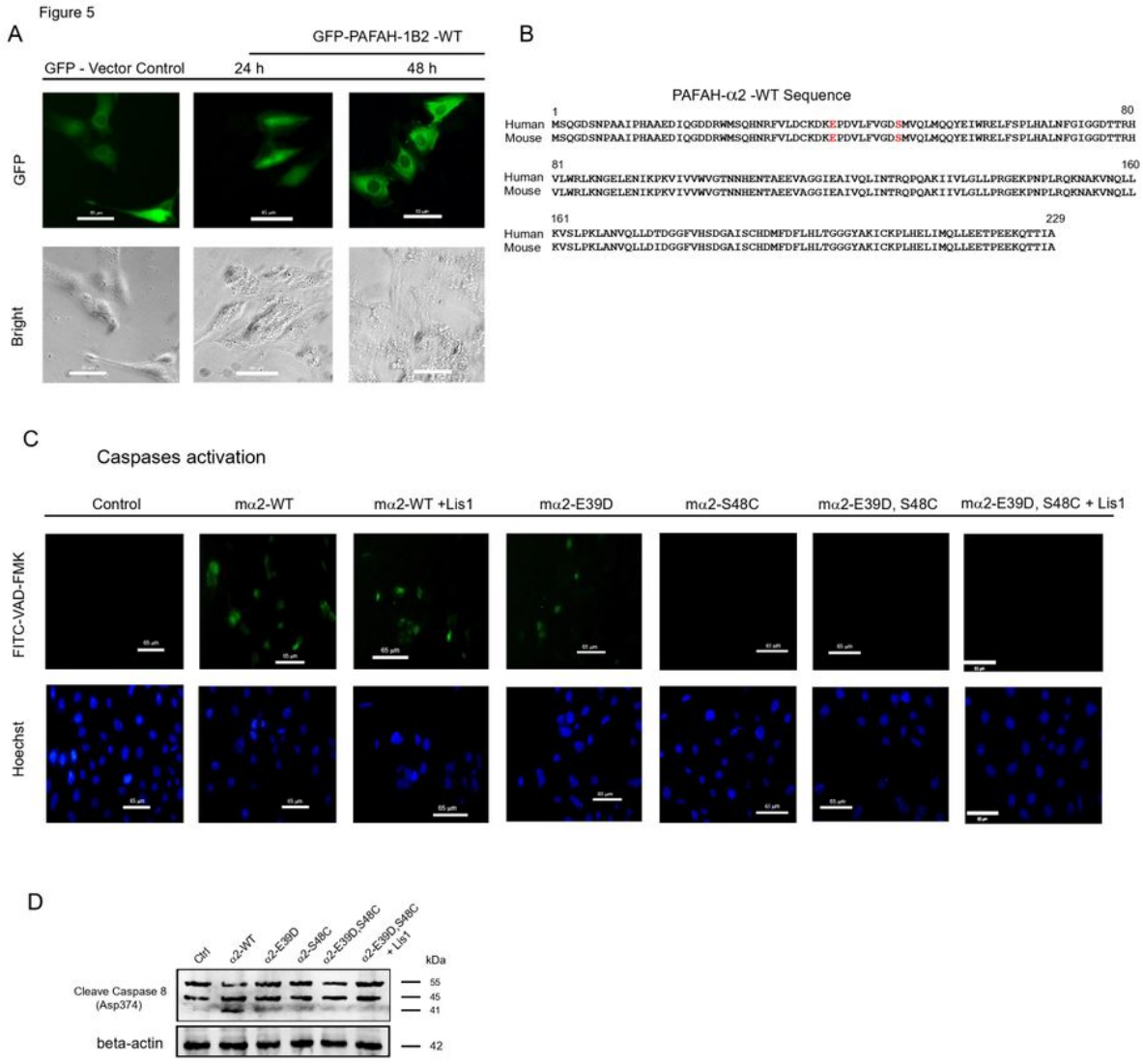

Figure 5

Overexpression of PAF-AH IB2 caused the caspase 8 activation and normal ovarian epithelium died. Human PAF-AH 1B2 WT transiently over-expression caused the HOSE sick and quickly died after 48-hour transfection (A). The blank vector linked with GFP was used as control. The protein sequence comparison between human and mouse (B). Detection caspase 8 activation with transfected with mouse PAF-AH 1B2

WT or enzymatic active site mutant (E39D, S48C) in living HOSE (C). Western blot validated the caspase 8 activation and cleavage in the HOSE with mouse PAF-AH 1B2 WT or mutant transfection (D).

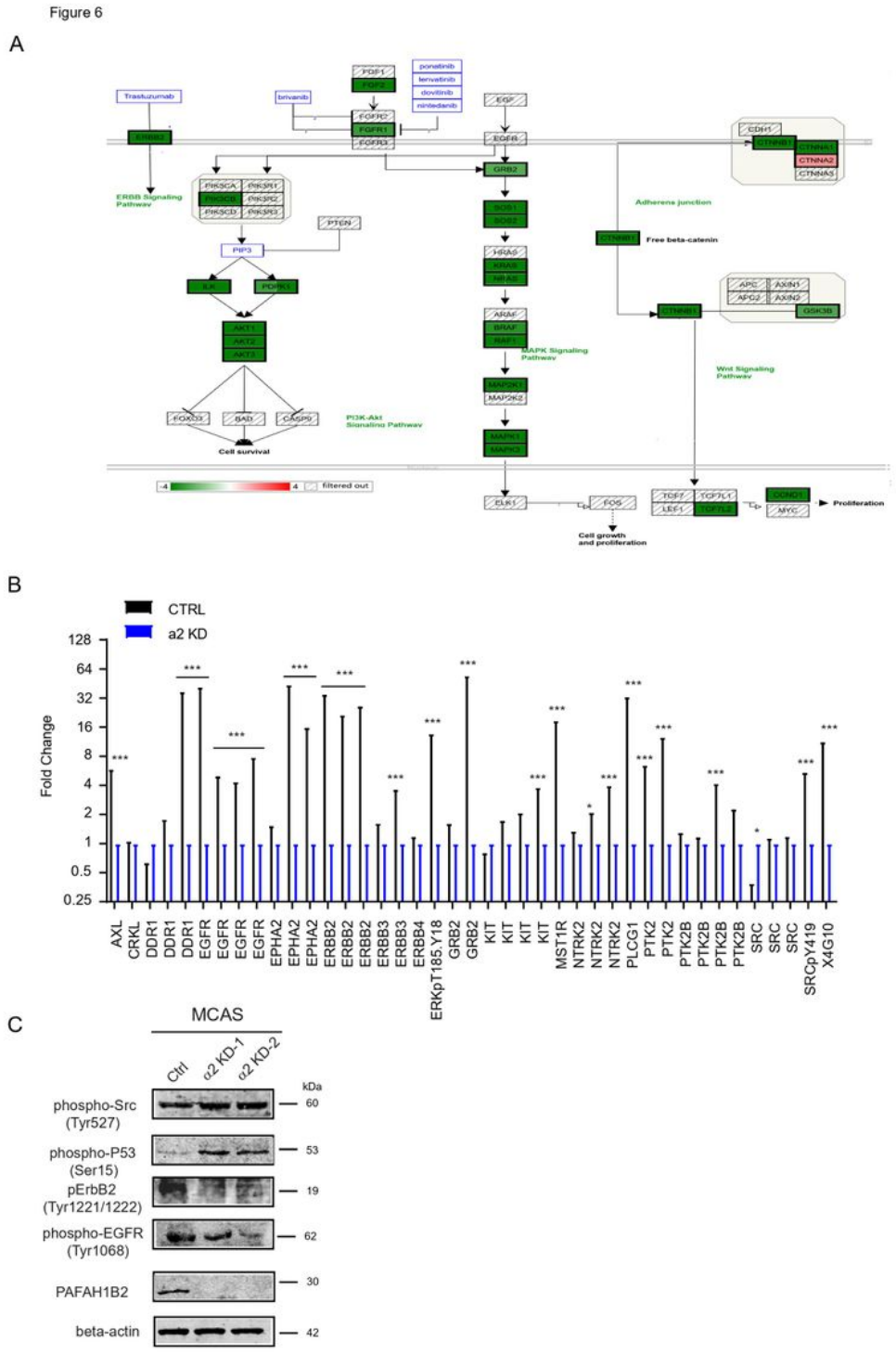

Figure 6

PAF-AH IB2 Knockdown decreased the growth factor kinase pathway in the ovarian cancer cell. The significantly changed genes in PAF-AH 1B2 KD MCAS cells were enriched in the growth factor kinase signalling pathway in endometrial cancer (A). Color indicates significantly up regulated signals and down

ward (green) ones indicate down regulated expression levels of the genes. Luminex immune-assay screen identified activated tyrosine kinases in PAF-AH 1B2 KD cancer cell lines (B). Western blot validated the signaling molecules change pattern in the PAF-AH 1B2 KD cells that involved in the epithermal growth factor kinase related signaling pathway (C).

Supplementary Files

This is a list of supplementary files associated with this preprint. Click to download.

- supplementaryfiles.pdf